Ultra-reliable Communication over Unreliable Optical Networks via Lightpath Diversity: System Characterization and Optimization

Yonggang Wen, *Student Member*, *IEEE* and Vincent W. S. Chan, *Fellow*, *IEEE*
Laboratory for Information and Decision Systems
Massachusetts Institute of Technology
Cambridge, MA, USA 02139
eewyg@mit.edu and chan@mit.edu

***Abstract*— We propose using diversity via multiple disjoint lightpaths at the optical layer to achieve ultra-reliable communication with low delay between any source-destination pair of all-optical networks. A Doubly-Stochastic Point Process model is used to characterize the photo-events of a direct detection receiver. The error probability can be designed to be significantly lower than that of a system without lightpath diversity. System parameters, such as the number of lightpaths used, are optimized to achieve efficient utilization of the limited optical transmitter power.**

Keywords-all-optical network; lightpath diversity; share-risk gourp; doubly-stochastic point process; symbol error probability

I. INTRODUCTION

When deployed, all-optical networks [1][2] will lead an architectural revolution for both long-haul and access networks. In all-optical networks, data traverse the network from source to destination without any optical-to-electrical conversion along the lightpath. During the past few years, optical networks have evolved from simple capacity expansion via wavelength-division multiplexing (WDM) to including other features, such as optical wavelength switching, dynamic reconfigurability and improved reliability. In this paper, we focus on the problem of providing ultra-high reliability for all-optical networks, which is crucial in many applications such as the interconnection of aircraft control systems.

In all-optical networks, communication between the transmitter and the receiver can be interrupted by failures that are located at different layers and/or interfaces between adjacent layers. To provide ultra-reliable communication in all-optical networks, two mechanisms can be used to counteract these failures: protection-switching and simultaneous lightpath-diversity.

Currently, the prevailing scheme is protection-switching approach, as implemented commercially in SONET-based optical networks. In this scheme, if a failure interrupts a source-destination connection, a detection algorithm locates the failure, and the connection is switched to another dedicated or shared backup lightpath. This scheme works well if the 50ms restoration time, specified by the SONET standard [3], is acceptable. However, due to the ultra-high data rate of optical networks (>10Gbps), a short-time interruption can result in a large amount of data loss. Furthermore, in some critical applications (e.g. when the network is used for transporting control signals between the cockpit and control surfaces in an aircraft), the time-deadline of control-message delivery needs to be shorter than 1-ms and probably ten times faster in failure detection. This is faster than the speed at which most optical components can switch. For these types of applications, the protection-switching mechanism cannot meet system requirements. Instead of increasing speeds of failure detection and lightpath switching to meet the increasing data rate and the critical time deadline, diversity via multiple disjoint lightpaths belonging to different shared-risk groups can provide reliable end-to-end data delivery in the presence of failures (e.g., fiber cuts and node crashes) [4][5].

For the system proposed here, the entire mechanism is implemented at the Physical Layer, and the network must be designed with a densely-connected physical topology such that there are multiple lightpaths between the source-destination pair [13]. For each channel symbol, the modulated light is split and sent through multiple independent lightpaths. At the receiver, received signals are combined optically before detection, or individually detected and electrically combined for symbol decisions. This allows a much faster response than protocols that provide end-to-end reliability at higher layers, such as TCP at the Transport Layer.

Moreover, as we will show, if the received signal-to-noise ratio (SNR) is high enough, the symbol error probability when using the maximal lightpath diversity is asymptotically equal to the probability of disconnecting the source-destination pair (i.e., we cannot find a connected path between the source-destination pair.) For any source-destination pair connected by M independent lightpaths, the asymptotic error probability is f^M where f is the individual lightpath failure probability. By choosing an optimal M, this limit can be made arbitrarily small compared to the asymptotic error probability of using a single path between the source-destination pair. This scheme requires network topologies with good all-terminal connectivity, which has been investigated intensively in [14].

The research in this paper is supported in part by Defense Advanced Research Projects Agency, Project MDA972-02-1-0021.

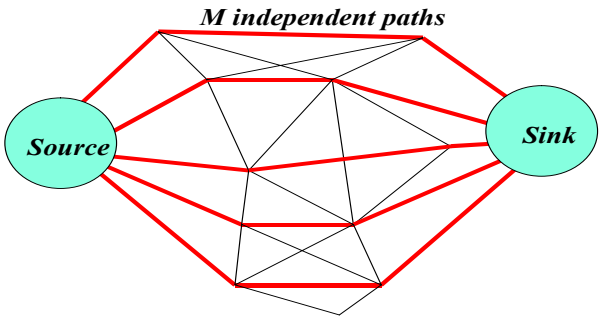

Fig. 1. Network model for an M-connected source-destination pair in densely-connected all-optical networks.

In this paper, we describe the lightpath-diversity network architecture and obtain a tight performance bound on the error probability, which is used to optimize overall system reliability. The remainder of this paper is organized as follows: In Section II, we formulate the detection problem and introduce the structured receiver architecture. As a benchmark, we characterize the error probability performance of the proposed system via an idealized receiver in Section III. In Section IV, the network is optimized via (1) minimizing the error probability for a given amount of transmitted power and (2) minimizing the transmitted power for a target error probability.

II. Problem Formulation

A. Network Model

We assume that the physical topology of the optical network has dense enough connections such that M independent lightpaths can always be found between source-destination pairs, as shown in Fig. 1 [13]. Physically, all the lightpaths must belong to different shared-risk groups to guarantee their independence. Each lightpath is modeled as an additive-noise channel with ON and OFF states. The OFF state corresponds to a disconnected lightpath and occurs with probability $f\,(0 \le f \le 1)$. The ON state occurs with probability $1-f$ and corresponds to a viable lightpath. Mathematically, the input-output relation of the channel can be expressed as $Y = FX + N$, as shown in Fig. 2, where X and Y are the input and the output, F is a Bernoulli random variable with $\Pr(F=0) = f$ and $\Pr(F=1) = 1-f$, and N is the additive noise (zero if no optical amplifier is used). For the source-destination pair, we define a lightpath state vector $\mathbf{F} = (F_1, F_2, \cdots, F_M)^T$, where F_i's are identical and independent Bernoulli random variables. The source-destination pair is also characterized by a delay vector $\boldsymbol{\tau} = (\tau_1, \tau_2, \cdots, \tau_M)^T$ and an attenuation vector $\mathbf{L} = (l_1, l_2, \cdots, l_M)^T$. For simplicity, we assume all the attenuation parameters are equal and normalized to one. Note that this result can be generalized to non-equal attenuation case by employing a corresponding optimal power allocation algorithm in the source node.

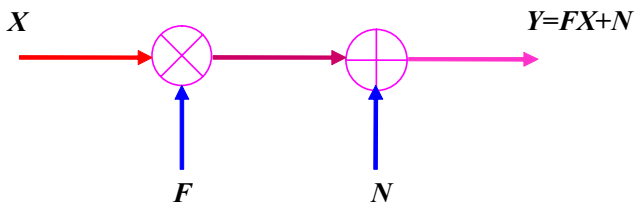

Fig. 2. Input-output model of an individual lightpath. X is the input, Y is the output, F is a Bernoulli random variable, and N is the noise.

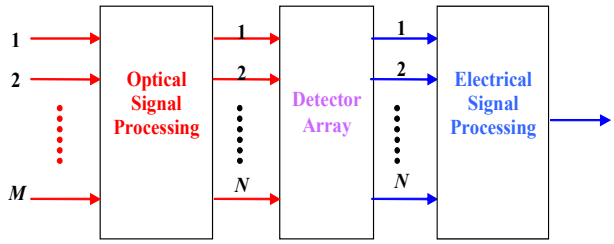

Fig. 3. Structured receiver architecture. It is separated into three cascaded modules: an optical signal processing module, an optical detection module and an electrical signal processing module.

Binary Pulse-Position Modulation (BPPM) is used to simplify the receiver implementation by not having to adaptively set the decision threshold as in the case of On-Off-Keying (OOK). The modulated signal is split into M parts. Each is sent over an independent lightpath to the receiver. With the assumption of identical and independent lightpaths, a uniform power allocation algorithm is optimal (See Appendix A). At the destination node, the receiver combines the M optical signals received over the disjoint lightpaths to make symbol-by-symbol decisions.

With direct detection, the photo-event count obeys Poisson statistics [6] if the optical signal is generated by a single-mode laser. The photo-event arrival rate λ (the number of photo-event per unit time) is determined by the received optical power. In our case, the received optical power is a random variable due to the random channel model. As a result, at the output of detectors, photo-event counting processes can be modeled as Doubly-Stochastic Point Processes [7].

B. Structured Receiver Architecture

We can design the optical receiver using two different approaches. Due to the quantum nature of weak optical signals, one method is to use a full quantum description of the receiver, and optimize it over the class of physically realizable measurements [8]. In this paper, we take a second "structured" or "semi-classical" approach [9]. These are not optimal quantum receivers but they are within a factor of two in energy efficiency of the optimum receiver for binary signaling. The infrastructure of all possible structured receivers can be separated into three cascaded processing modules as illustrated in Fig. 3: an optical signal processing module, an optical detection module, and an electrical signal processing module. The three modules must be jointly optimized to achieve a globally optimum performance.

III. System Characterizations

In this section, we characterize the lightpath-diversity scheme with a tight upper bound on the symbol error probability. We assume that an idealized receiver obtains the lightpath state vector $\mathbf{F}$ from a "genie". At the optical signal processing module, M optical delay lines are used to

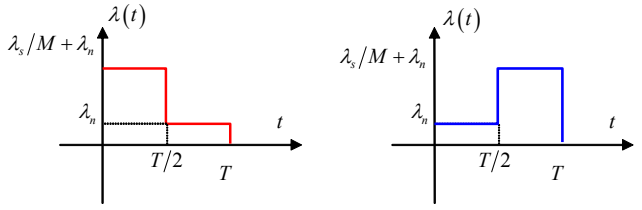

Fig. 4. Detected photo-event rates for two hypotheses with BPPM signal when the lightpath is ON.

compensate the delay variations among the M disjoint lightpaths (Since we use M parallel detectors, fiber delay can also be replaced by time delay in the electrical signal processing stage). At the optical detection module, the photo-events at the output of M direct detectors are recorded for symbol decisions. At the electrical module, the Maximum Likelihood (ML) decision rule is applied to the vector output of the detectors to make optimal symbol decisions.

A. *Photo-event Counting Process*

With the BPPM signaling and uniform power allocation, the transmitted power over the i^{th} lightpath is

$$P_i^{(0)}(t)=\begin{cases}P_s/M & 0\le t\le T/2\\ 0 & T/2\le t\le T\end{cases} \tag{1}$$

under hypothesis H_0 (i.e., symbol "0"), and the transmitted power over the i^{th} lightpath is

$$P_i^{(1)}(t)=\begin{cases}0 & 0\le t\le T/2\\ P_s/M & T/2\le t\le T\end{cases} \tag{2}$$

under hypothesis H_1 (i.e., symbol "1"). In both cases, P_s is the average output power of the laser.

If there is no noise in fiber channel, under hypothesis H_0, the recorded photo-event rate at the output of the i^{th} detector is given by

$$\lambda_i^{(0)}(t)=\begin{cases}F_i\lambda_s/M & 0\le t\le T/2\\ 0 & T/2\le t\le T\end{cases}. \tag{3}$$

Under hypothesis H_1, the recorded photo-event rate at the output of the i^{th} detector is

$$\lambda_i^{(1)}(t)=\begin{cases}0 & 0\le t\le T/2\\ F_i\lambda_s/M & T/2\le t\le T\end{cases}. \tag{4}$$

In both cases, $\lambda_s=\eta P_s/h\nu$ (η is the detector quantum efficiency, $h\nu$ is the photon energy) is the rate parameter of the photo-event counting process. The received optical signals can be corrupted by amplifier noises if optical amplifiers are used. We assume that the noise process receives contributions from many spatial-temporal modes and the probability of two successive photo-events coming from the same spatial-temporal mode is close to zero. In this case, the Weak Photon-Coherence Assumption holds, and we can approximate the noise-driven photo-event counting process by a Poisson Process with a constant rate λ_n equal to its mean arrival rate. Combining (3) and (4), the photo-event counting process has a random arrival rate $F_i\lambda_i^{(j)}(t)+\lambda_n$ for given hypothesis H_j, as shown in Fig. 4 for $F_i=1$. It follows that recorded photo-event counting processes can be modeled as Doubly-Stochastic Point Processes.

B. *Optimum Decision Rule*

If $m\le M$ lightpaths are ON during the symbol duration, we can re-index them from 1 to m for a genie-aided receiver. Under this scenario, the optimal decision rule is the same as the detection rule for the scenario with m perfectly reliable lightpaths [7], i.e.,

$$\sum_{i=1}^{m}k_{i1}\underset{\widehat{H}=H_1}{\overset{\widehat{H}=H_0}{\gtrless}}\sum_{i=1}^{m}k_{i2}, \tag{5}$$

where k_{i1} and k_{i2} are the number of photo-events recorded during $[0,T/2]$ and $[T/2,T]$ over the i^{th} lightpath, respectively.

C. *System Characterization: Error Probability Bound*

In this subsection, we derive a tight upper bound on the error probability for the genie-aided receiver via a two-step procedure: (1) the upper bound of the conditional error probability on the number of ON lightpaths is calculated, and then (2) the overall error probability upper bound is calculated by averaging the conditional error probability bound over the distribution of the number of ON lightpaths.

Given that m lightpaths are ON during the transmission, the conditional error probability is given by

$$\begin{aligned}\Pr(\varepsilon\mid m)&=P_0\Pr\left[\sum_{i=1}^{m}k_{i1}\le\sum_{i=1}^{m}k_{i2}\mid H_0,m\right]\\&\quad+P_1\Pr\left[\sum_{i=1}^{m}k_{i1}\ge\sum_{i=1}^{m}k_{i2}\mid H_1,m\right]\\&=\Pr\left[\sum_{i=1}^{m}k_{i1}\le\sum_{i=1}^{m}k_{i2}\mid H_0,m\right],\end{aligned} \tag{6}$$

where the second equality is due to the symmetry of binary pulse-position modulation and $P_0=P_1=1/2$ for equiprobable digital source . Since a closed form solution of $\Pr(\varepsilon\mid m)$ is not available, we use the exponentially tight Chernoff upper bound [10], that is,

$$\begin{aligned}\Pr\left[\sum_{i=1}^{M}k_{i1}\le\sum_{i=1}^{M}k_{i2}\mid H_0,m\right]&\le E_{s>0}\left\{e^{s\left(\sum_{i=1}^{M}k_{i2}-\sum_{i=1}^{M}k_{i1}\right)}\mid H_0,m\right\}\\&=\exp\left\{mN_n\left(e^{s}-1\right)+\left(\frac{mN_s}{M}+mN_n\right)\left(e^{-s}-1\right)\right\},\end{aligned} \tag{7}$$

where $N_s = T\lambda_s/2$ and $N_n = T\lambda_n/2$ are the number of data-driven and noise-driven photo-events recorded over a period of $T/2$. Since the inequality is valid for any value of $s > 0$, the bound can be tightened by minimizing right hand side of (7),

$$\Pr(\varepsilon \mid m) \le \min_{s>0} \exp\left\{ mN_n\left(e^s - 1\right) + \left(\frac{mN_s}{M} + mN_n\right)\left(e^{-s} - 1\right)\right\}$$
$$= \exp\left\{ -m\left(\sqrt{\frac{N_s}{M} + N_n} - \sqrt{N_n}\right)^2 \right\}, \quad (8)$$

where the minimum is achieved if and only if $e^s = \sqrt{1 + N_s/(MN_n)}$.

The overall error probability is then obtained by averaging the conditional error probability (8) over the distribution of m,

$$\Pr(\varepsilon) = \sum_{m=0}^{M} \Pr(\varepsilon \mid m)\Pr(m). \quad (9)$$

Let $m = \sum_{i=1}^{M} F_i$ be the number of ON lightpaths. Note that m has the binomial distribution, i.e.,

$$\Pr\{m\} = \frac{M!}{m!(M-m!)}(1-f)^m f^{M-m}. \quad (10)$$

Substituting (8) and (10) into (9), we obtain

$$\Pr(\varepsilon) \le \sum_{m=0}^{M} \frac{M!}{m!(M-m)!}(1-f)^m f^{M-m} e^{-m\psi(N_s,N_n,M)} \triangleq PB_{GA}, \quad (11)$$

where $\psi(N_s, N_n, M) = \left(\sqrt{N_s/M + N_n} - \sqrt{N_n}\right)^2$. The right hand side of (11) has the form of the characteristic function of the random variable m. Using the fact that the characteristics function of a binomial random variable $X \sim B(n, 1-f)$ is $\left(f + (1-f)e^{jv}\right)^n$ [11], we obtain the overall error probability upper-bound as

$$PB_{GA} = \left[f + (1-f)e^{-\psi(N_s,N_n,M)} \right]^M. \quad (12)$$

For sanity check, if $f = 0$, (12) turns out to be

$$PB_{GA} = \exp\left\{ -\left(\sqrt{N_s + MN_n} - \sqrt{MN_n}\right)^2 \right\}, \quad (13)$$

which is the error probability bound for the source-destination pair connected by M reliable lightpaths.

The error probability upper-bound (12) is plotted in Fig. 5. In the high SNR regime, the error probability curves converge to error floors. These floors are due to the event that the source-destination pair is disconnected, and are thus equal to f^M. It suggests that a network topology with high all-terminal connectivity is preferable [14]. In the medium SNR regime, the error performance depends highly on the number of lightpaths for a given amount of power. This indicates that we can optimize the number of lightpaths to achieve an efficient utilization of the transmitted power. We would avoid working in the low SNR regime due to its poor error performance.

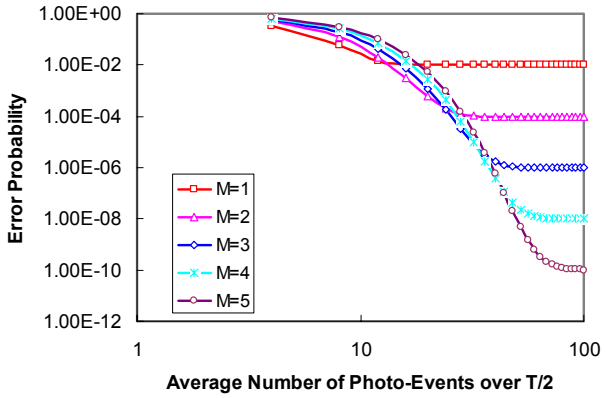

Fig. 5. The error probability bound for the idealized receiver with different number of lightpaths. $f = 0.01, N_n = 2$.

IV. System Optimizations

The output power of the transmitter is limited by physical constraints such as laser construction. To utilize this amount of power efficiently, we optimize the system for different objective functions over the choice of network parameters, such as the number of lightpaths used.

A. Minimizing the Error Probability

Given a limited amount of transmitter power, the number of lightpaths used can be optimized to minimize the error probability. Mathematically, this is equivalent to solving the following nonlinear programming problem,

$$\min \quad G(M) = \left(f + (1-f)e^{-\psi(N_s,N_n,M)}\right)^M$$
$$s.t. \quad M \in \mathbb{N}(\text{the set of positive integers}). \quad (14)$$

Instead of finding the exact solution, we relax the integer constraint, and assume M is a positive real number to solve the approximate problem without the integer constraint. Note that the minimum of $G(M)$ without the integer constraint is a lower bound of the minimum of $G(M)$ with the integer constraint. In the low SNR regime, we want to use only a few lightpaths. In the high SNR regime, we want to use as many lightpaths as possible. In the medium SNR regime with $0 < f < 1/2$, the optimum of M^* (See Appendix B) is approximated by

$$M^* \approx \frac{N_s}{\zeta(f, N_n)}, \quad (15)$$

where $\zeta(f, N_n) = \ln(1/f - 1) + 2\sqrt{N_n}\sqrt{\ln(1/f - 1)} > 0$. This result indicates that the optimum M^* increases linearly with the transmitted power N_s with a slope of $1/\zeta(f, N_n)$, and each lightpath requires an optimal average number of photo-

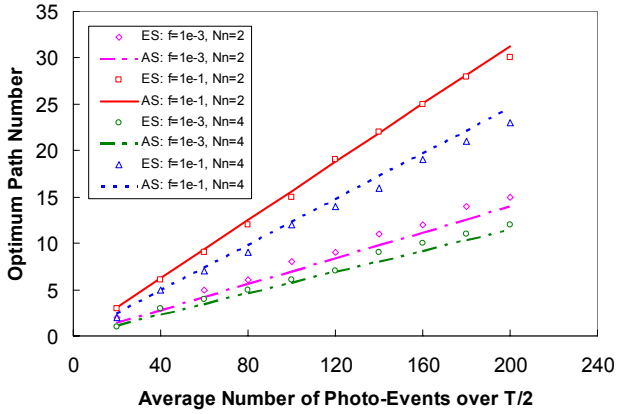

Fig. 6. The optimal number of lightpaths used is plot against different signal power levels. As a reference, we also plot results from the exhaustive search. ES: exhaustive search, AS: analytical solution.

events $\zeta\left(f, N_n\right)$ determined by f and N_n. For comparison, we have also found the optimal integer M^* by using an exhaustive search algorithm. In Fig. 6, the results from both the exhaustive search algorithm (bullets) and the analytical solution (lines) are plotted against different power levels, i.e., the average number of photo-events over duration of $T/2$. The analytical results match the numerical results well, and the slope, M^*/N_s, is a monotonically increasing function of f.

By substituting (15) into (12), the error probability bound is approximated by,

$$PB_{GA} \approx \exp\left\{-N_s \Theta\left(f, N_n\right)\right\}, \tag{16}$$

where $\Theta\left(f, N_n\right) = -\ln\left(2f\right)/\zeta\left(f, N_n\right) > 0$ for $0 < f < 1/2$.
The error exponent decreases linearly as the transmitted power with a slope of $-\Theta\left(f, N_n\right)$, as shown in Fig. 7.

B. *Minimizing the Total Transmitted Power*

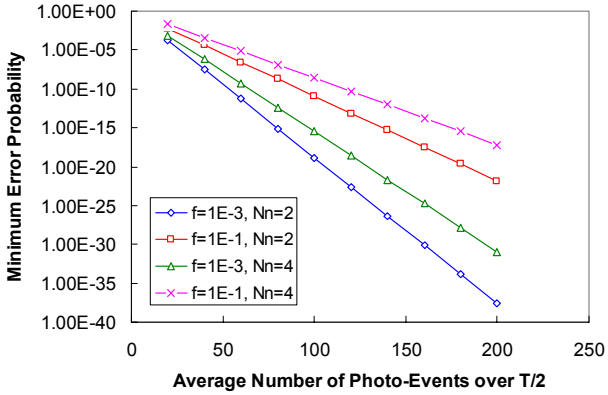

Fig. 7. The minimum error probability with a given power is plot against different signal power levels (i.e., the average number of recorded photo-event over a period of $T/2$).

In this subsection, we minimize the total transmitted power for a target error probability. In the low SNR regime, we want to use as few lightpaths as possible, but still satisfy the requirement of $P_b \geq f^M$. It follows that the optimal number of lightpaths is given by $M^\dagger = \lceil \ln P_b / \ln f \rceil$. In the high SNR regime, the optimum number of lightpaths is the same as the maximal number of available lightpaths. Both cases are trivial. For the medium SNR regime, the solution is derived as follows.

For a given amount of transmitted power N_s, from (16), the error probability is approximated by

$$P_b = \exp\left\{-N_s \Theta\left(f, N_n\right)\right\}. \tag{17}$$

Using (17), for a given P_b, the minimum optical power required is given by

$$N_s^\dagger = \frac{\ln\left(1/P_b\right)}{\Theta\left(f, N_n\right)}. \tag{18}$$

(18) suggests that the minimum transmitted power decreases

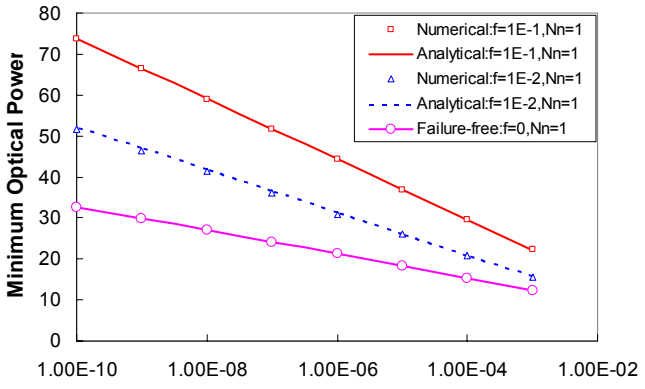

(a)

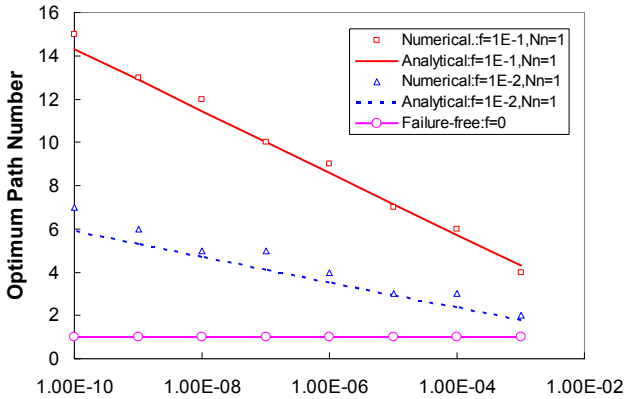

(b)

Fig. 8. (a) The minimum total transmitted power for various required error probabilities. ES: exhaustive search, AS: analytical solution; (b) The optimum number of paths to minimize the total transmitted power is plot against various target error probabilities.

linearly with the log of the error probability with a slope of $1/\Theta(f, N_n)$, as shown in Fig. 8(a) for both analytical and numerical solutions.

By substituting (18) into (15), the optimal number of lightpaths to minimize the transmitted power is given by

$$M^{\dagger} = \frac{\ln P_b}{\ln(2f)} \quad (19)$$

(19) indicates that the optimal number of lightpaths decreases linearly with the log of the error probability with a slope of $1/\ln(2f) < 0$, as shown in Fig. 8(b).

V. CONCLUSION

In this paper, we proposed the use of lightpath-diversity to achieve ultra-reliable end-to-end communication in all-optical networks. For a network with dense connections, arbitrary reliability can be achieved if enough independent lightpaths are used. Since this approach is implemented entirely at the Physical Layer without the use of higher layer protocol such as ARQ's, the response will be fast enough for applications with critical time deadlines. From a theoretical perspective, we have characterized the proposed lightpath-diversity system with a Doubly-Stochastic Point Process model. The fundamental limit on the error probability of the scheme has been obtained via a genie-aided receiver. This fundamental error metric could serve as a benchmark for other receiver architectures. Under typical operating scenarios, we have also optimized the system performance by choosing an optimal number of lightpaths used to utilize the limited optical power efficiently with different objective functions.

From an engineering perspective, we will investigate the class of all structured receivers and explore the trade-off between the implementation complexity and the error probability in future research.

APPENDIXES

A. Optimum Power Allocation Algorithm

For an M-connected source-destination pair, the power allocation vector is $\mathbf{P} = (N_1, N_2, \ldots, N_M)^T$, and the state vector is $\mathbf{F} = (F_1, F_2, \cdots, F_M)^T$ with a probability distribution of $\Pr(\mathbf{F}) = f^{\sum_{i=1}^{M} F_i} (1-f)^{M - \sum_{i=1}^{M} F_i}$. For the genie-aided receiver, the overall error probability upper-bound is given by

$$PB_{GA} = \sum_{\mathbf{F} \in \{0,1\}^M} \Pr(\mathbf{F}) e^{-\left(\sqrt{\mathbf{F}^T(\mathbf{P}+\mathbf{N}_n)} - \sqrt{\mathbf{F}^T \mathbf{N}_n}\right)^2} \quad (A.1)$$

where $\mathbf{N}_n = (N_n, N_n, \ldots, N_n)^T$ is the noise power vector and $\{0,1\}^M$ is the M-dimensional vector space over $\{0,1\}$ field.

To minimize the error probability, we solve the following nonlinear programming problem,

$$\begin{aligned} \min \quad & h(\mathbf{P}) = \sum_{\mathbf{F} \in \{0,1\}^M} \Pr(\mathbf{F}) e^{-\left(\sqrt{\mathbf{F}^T(\mathbf{P}+\mathbf{N}_n)} - \sqrt{\mathbf{F}^T \mathbf{N}_n}\right)^2} \\ s.t. \quad & \mathbf{P}^T \mathbf{1} = N_s \end{aligned} \quad (A.2)$$

where $\mathbf{1} = (1, 1, \ldots, 1)^T$.

From the fact that, for each $\mathbf{F} = (F_1, F_2, \cdots, F_M) \in \{0,1\}^M$, the function $\exp\left\{-\left(\sqrt{\mathbf{F}^T(\mathbf{P}+\mathbf{N}_n)} - \sqrt{\mathbf{F}^T \mathbf{N}_n}\right)^2\right\}$ is a convex function defined over a compact convex set $\left\{(N_1, N_2, \ldots, N_M) : \sum_{i=1}^{M} N_i = N_s\right\}$, the minimization problem (A.2) has a unique solution.

From the Karush-Kuhn-Tuck conditions [12], we obtain

$$\nabla_{\mathbf{P}} L(\mathbf{P}, \mu) = 0, \quad (A.3)$$

where $L(\mathbf{P}, \mu) = h(\mathbf{P}) - \mu(\mathbf{P}^T \mathbf{1} - N_s)$, and μ is the Lagrange multiplier. From (A.3), the optimum power allocation vector is given by

$$\mathbf{P} = \left(\frac{N_s}{M}, \frac{N_s}{M}, \ldots, \frac{N_s}{M}\right)^T \quad (A.4)$$

(A.4) indicates that the uniform power allocation algorithm is optimal under the assumption of identical and independent multiple lightpaths.

B. Optimum Number of Total Paths

In this subsection, we solve the nonlinear programming problem given by

$$\min_{M>0} G(M) = \left(f + (1-f)\exp\{-\psi(N_s, N_n, M)\}\right)^M \quad (B.1)$$

From the Implicit Function Theorem [12], there exists a function $M^* = g(N_s, N_n, f)$ such that $G(M)$ is minimized over the convex set $\{M : M \in \mathbb{R}^+\}$. We find an approximation of the function $M^* = g(N_s, N_n, f)$ as follows.

Let $a = f$ and $b(M) = (1-f)\exp\{-\psi(N_s, N_n, M)\}$. Note that $0 \le a, b(M) \le 1$ and $G(M) = (a + b(M))^M$. To first order approximation in the medium SNR regime, the optimum number M^* of lightpaths can be approximated by the value of M with which the curve a^M and the curve b^M meet, i.e.,

$$a^M = b(M)^M \quad (B.2)$$

If $0 < f < 0.5$, (B.2) has a unique solution given by

$$M^* = \frac{N_s}{\ln\left(\frac{1-f}{f}\right) + 2\sqrt{N_n}\sqrt{\ln\left(\frac{1-f}{f}\right)}} \quad (B.3)$$

This approximation is found to be very good when compared to a numerical search for M^*.

ACKNOWLEDGEMENT

The authors wish to thank Muriel Medeard, Poompat Saengudomlert, Yueh-Ping Lim, Jihwan Choi, Lillian Dai, Chunmei Liu, and Jun Sun for the helpful discussions.

REFERENCES

[1] V. W. S. Chan, et al, "A precompetitive consortium on wide-band all-optical networks," IEEE/LEOS Journal of Lightwave Technology, Vol. 11, No. 5/6, May/June, 1993, pp. 714-735.

[2] V. W. S. Chan, "All-Optical Networks," Scientific American 273, No. 3, September 1995, pp. 56-59.

[3] "Architecture of Optical Transport Networks", ITU-T Recommendation G. 872, Feb. 1999.

[4] V. W. S. Chan and A. H. Chan, "Reliable Message Delivery via Unreliable Networks," 1997 IEEE International Symposium on Information Theory, Ulm, Germany, 29 June - 4 July 1997.

[5] Salil Parikh, *On the Use of Erasure Codes in Unreliable Data Network*, M.Sc. Thesis, MIT, May 2001.

[6] I. Bar-David, "Communication under the Poisson Regime", IEEE Transaction on Information Theory, Vol. IT-15, No. 1, January 1969, pp. 31-37.

[7] D. L. Snyder, *Random Point Processes*, by John Wiley & Sons, Inc., 1975.

[8] C. W. Helstrom and R. S. Kennedy, "Noncommuting Observables in Quantum Detection and Estimation Theory", IEEE Transaction on Information Theory, Vol. IT-20, No.1, January 1974, pp.16-24.

[9] S. Karp and J. R. Clark, "Photon Counting: a Problem in Classical Noise Theory", IEEE transaction on information theory, Vol. IT-16, November 1970, pp. 672-680.

[10] H. L. Van Trees, *Detection, Estimation and Modulation Theory*, Part I, John Wiley, New York, 1968.

[11] D. P. Bertsekas and J. N. Tsitsiklis, *Introduction to Probability*, Athena Scientific, Belmont, Massachusetts, 2002.

[12] D. P. Bertsekas, *Nonlinear Programming*, 2nd edition, Athena Scientific, Belmont, Massachusetts, 1999.

[13] G. Weichenberg, High-Reliability Architectures for Networks under Stress, M.Sc. Thesis, EECS, MIT, 2003.

[14] G. Weichenberg, Vincent W. S. Chan, and Muriel Medard, "High-Reliability Architectures for Networks under Stress," DRCN 2003.